SANDIA REPORT

SAND2012-8910
Unlimited Release
Printed October 2012

Adjoint Based a posteriori Error Estimation in Drekar::CFD

Timothy M. Wildey, Eric C. Cyr, Roger Pawlowski, John N. Shadid, and Tom M. Smith

Prepared by
Sandia National Laboratories
Albuquerque, New Mexico 87185 and Livermore, California 94550

Sandia National Laboratories is a multi-program laboratory managed and operated by Sandia Corporation, a wholly owned subsidiary of Lockheed Martin Corporation, for the U.S. Department of Energy's National Nuclear Security Administration under contract DE-AC04-94AL85000.

Approved for public release; further dissemination unlimited.

Sandia National Laboratories

Issued by Sandia National Laboratories, operated for the United States Department of Energy by Sandia Corporation.

NOTICE: This report was prepared as an account of work sponsored by an agency of the United States Government. Neither the United States Government, nor any agency thereof, nor any of their employees, nor any of their contractors, subcontractors, or their employees, make any warranty, express or implied, or assume any legal liability or responsibility for the accuracy, completeness, or usefulness of any information, apparatus, product, or process disclosed, or represent that its use would not infringe privately owned rights. Reference herein to any specific commercial product, process, or service by trade name, trademark, manufacturer, or otherwise, does not necessarily constitute or imply its endorsement, recommendation, or favoring by the United States Government, any agency thereof, or any of their contractors or subcontractors. The views and opinions expressed herein do not necessarily state or reflect those of the United States Government, any agency thereof, or any of their contractors.

Printed in the United States of America. This report has been reproduced directly from the best available copy.

Available to DOE and DOE contractors from
U.S. Department of Energy
Office of Scientific and Technical Information
P.O. Box 62
Oak Ridge, TN 37831

Telephone: (865) 576-8401
Facsimile: (865) 576-5728
E-Mail: reports@adonis.osti.gov
Online ordering: http://www.osti.gov/bridge

Available to the public from
U.S. Department of Commerce
National Technical Information Service
5285 Port Royal Rd
Springfield, VA 22161

Telephone: (800) 553-6847
Facsimile: (703) 605-6900
E-Mail: orders@ntis.fedworld.gov
Online ordering: http://www.ntis.gov/help/ordermethods.asp?loc=7-4-0#online

SAND2012-8910
Unlimited Release
Printed October 2012

Adjoint Based a posteriori Error Estimation in Drekar::CFD

Timothy M. Wildey, Eric C. Cyr, Roger Pawlowski,
John N. Shadid, and Tom M. Smith
Sandia National Laboratories
P.O. Box 5800
Albuquerque, NM 87185-1318
tmwilde@sandia.gov, eccyr@sandia.gov, rppawlo@sandia.gov,
jnshadi@sandia.gov, tmsmith@sandia.gov

Abstract

This document summarizes the results from a level 3 milestone study within the CASL VUQ effort. It demonstrates the capability to perform adjoint-based a posteriori error estimation within Drekar::CFD. The a posteriori error estimates require the solution of a (linear) adjoint problem in a higher order approximation space with data chosen based on the quantity of interest. The a posteriori error estimates are verified using an analytical solution to a laminar flow problem. Finally, the framework is demonstrated on the TH-M Test Case #2 involving a 3-dimensional axisymmetric sudden expansion with a moderate Reynolds numbers (5000).

Acknowledgment

The authors thank Tom Smith for delivering the thermal hydraulics examples used in this study.

Contents

1 Background . . . 7
2 Adjoint Based Error Analysis . . . 8
2.1 General Nonlinear Problem and Notation . . . 8
2.2 Strong Form Adjoint Operators . . . 8
2.3 Variational Formulation . . . 9
2.4 Stabilized Formulations . . . 9
2.5 Navier-Stokes . . . 10
3 Drekar Implementation . . . 12
4 Computational Experiments . . . 14
4.1 Channel Flow . . . 14
4.2 Axisymmetric Expansion . . . 16
5 Observations . . . 21
References . . . 22

Figures

1 Magnitude of the forward velocity for the channel verification problem. . . . 14
2 Magnitude of the adjoint velocity corresponding to QofI 2 for Re= 10 (left) and for Re=1000 (right). . . . 16
3 The adjoint pressure for Re= 10 corresponding to QofI 1 (left) and to QofI 3 (right). 16
4 Computational mesh for the axisymmetric sudden expansion problem. . . . 17
5 Magnitude of the forward velocity corresponding to Re= 500. . . . 17
6 Magnitude of the adjoint velocity (left) and the adjoint pressure (right) corresponding to the average x-velocity over the domain. . . . 19
7 Magnitude of the adjoint velocity (left) and the adjoint pressure (right) corresponding to the value of the z-velocity at (0,0,0). . . . 19
8 Magnitude of the adjoint velocity (left) and the adjoint pressure (right) corresponding to the average value of the z-velocity over $[-0.03, 0.03] \times [-0.03, 0.03] \times [0.02, 0.03]$.. . . . 20

Tables

1 Error estimates and effectivity ratios for the three quantities of interest with Re= 10 and Re=1000. . . . 15
2 Error estimates for the quantities of interest for the axisymmetric sudden expansion problem. . . . 18
3 Error estimates for a quantity of interest using an SA-RANS approximation of the axisymmetric sudden expansion problem. . . . 20

1 Background

A posteriori error estimates have become a common means to quantify the reliability of predictions from numerical simulations. This methodology has been developed for a large number of methods and is widely accepted in the analysis of discretization error for partial differential equations [1, 9, 10]. The adjoint-based (dual-weighted residual) method, is motivated by the observation that oftentimes the goal of a simulation is to compute a small number of linear functionals of the solution, such as the average value in a region or the drag on an object, rather than controlling the error in a global norm. This method has been successfully extended to estimate numerical errors due to operator splittings [11] and operator decomposition for multiscale/multiphysics applications [6, 15, 16]. adaptive sampling algorithms [13, 14], stochastic approximations [20, 4], and inverse sensitivity analysis [3, 5].

Despite their wide applicability and attractive features, adjoints have not become common in production software packages. In large part, this is due to the computational cost required to set up and solving the adjoint problem. This is especially problematic for nonlinear time-dependent problems. The goal of this milestone is to demonstrate the ability to define and solve adjoint problems in Drekar::CFD and produce accurate a posteriori error estimates for a variety of quantities of interest. We focus on steady-state solutions to the Navier-Stokes equations discretized using stabilized continuous Galerkin finite elements. Future work will build upon the capabilities developed in this effort and will extend the capabilities in Drekar::CFD to address/mitigate some of the challenges in adjoint simulations.

2 Adjoint Based Error Analysis

2.1 General Nonlinear Problem and Notation

We consider the following system of partial differential equations,

$$\boldsymbol{F}(\boldsymbol{z}) = \boldsymbol{0}, \tag{1}$$

defined on $\Omega \subset \mathbb{R}^d$, $d = 2,3$, a polygonal (polyhedral) domain (open, bounded, and connected set) with boundary $\partial\Omega$. Specific examples of $\boldsymbol{F}$ and $\boldsymbol{z}$ will be given in subsequent sections. We assume that sufficient boundary conditions are provided so that (1) is well-posed. We present the definition of the adjoint problem and the a posteriori error analysis using the general problem formulation (1). In section 2.5, we provide specific formulations for the Navier Stokes equations as an example. We remark that our general approach can also be used for RANS models, LES models, and thermal hydraulics, but these specific formulations are omitted for the sake of brevity.

2.2 Strong Form Adjoint Operators

The goal in adjoint-based error analysis is to relate a linear (or linearized) functional of the error to a computable weighted residual. The linear adjoint operator in strong form can be defined via the duality relation

$$(\mathscr{L}\boldsymbol{v}, \boldsymbol{w}) = (\boldsymbol{v}, \mathscr{L}^*\boldsymbol{w}) \tag{2}$$

where $\mathscr{L}$ is a linear operator. For a general nonlinear PDE one approach to define the linear operator $\mathscr{L}$ is to assume $\boldsymbol{F}$ is convex and use the Integral Mean Value Theorem yielding

$$\boldsymbol{F}'(\bar{\boldsymbol{z}})\boldsymbol{e} = \boldsymbol{F}(\boldsymbol{z}) - \boldsymbol{F}(\boldsymbol{z}_h)$$

where $\bar{\boldsymbol{z}}$ lies on the line connecting $\boldsymbol{z}$ and $\boldsymbol{z}_h$, and $\boldsymbol{e} = \boldsymbol{z} - \boldsymbol{z}_h$. In practice, $\bar{\boldsymbol{z}}$ is unknown so we linearize around $\boldsymbol{z}_h$ giving,

$$\mathscr{L}\boldsymbol{e} = \boldsymbol{F}'(\boldsymbol{z}_h)\boldsymbol{e} = \boldsymbol{F}(\boldsymbol{z}) - \boldsymbol{F}(\boldsymbol{z}_h) + h.o.t.$$

Notice that the operator $\mathscr{L}$ is the same linear operator used in computing the step in Newton's method. This fact is often exploited to ease construction of the discrete adjoint operator.

For the linear functional denoted by the duality pairing $(\boldsymbol{\psi}, \cdot)$ the error can be represented using the definition of the adjoint. We follow the standard approach and neglect the higher order terms in the error representation, see e.g. [2, 1, 12, 16], giving

$$(\boldsymbol{\psi}, \boldsymbol{e}) = (\boldsymbol{\psi}, \mathscr{L}^{-1}(\boldsymbol{F}(\boldsymbol{z}) - \boldsymbol{F}(\boldsymbol{z}_h)) = (\boldsymbol{\phi}, \boldsymbol{F}(\boldsymbol{z}) - \boldsymbol{F}(\boldsymbol{z}_h)) \tag{3}$$

where $\boldsymbol{\phi}$ is defined by the adjoint problem

$$\mathscr{L}^*\boldsymbol{\phi} = \boldsymbol{\psi}. \tag{4}$$

2.3 Variational Formulation

We assume that (1) has an equivalent variational formulation seeking $\boldsymbol{z} \in \boldsymbol{V}$ such that,

$$\boldsymbol{f}(\boldsymbol{z}, \boldsymbol{w}) = \boldsymbol{0}, \quad \forall \boldsymbol{w} \in \boldsymbol{V}. \tag{5}$$

Note that $\boldsymbol{f}$ is assumed to be linear $\boldsymbol{w}$. Specific examples of $\boldsymbol{f}$ and $\boldsymbol{V}$ will be given in subsequent sections. The discrete problem is defined by choosing $\boldsymbol{V}_h \subset \boldsymbol{V}$ to be a discrete subspace associated with the partition, $\mathscr{T}_h$, and letting $\boldsymbol{z}_h \in \boldsymbol{V}_h$ satisfy,

$$\boldsymbol{f}(\boldsymbol{z}_h, \boldsymbol{w}) = \boldsymbol{0}, \quad \forall \boldsymbol{w} \in \boldsymbol{V}_h. \tag{6}$$

This statement combined with the linearity in $\boldsymbol{w}$ is equivalent to *Galerkin orthogonality*, and in what follows we will refer to these interchangeably.

Deriving the adjoint of the variational formulation follows the same pattern as the strong-form operator. To define the error representation the Integral Mean Value Theorem is again applied giving

$$\boldsymbol{f}'(\bar{\boldsymbol{z}}; \boldsymbol{e}, \boldsymbol{w}) = \boldsymbol{f}(\boldsymbol{z}, \boldsymbol{w}) - \boldsymbol{f}(\boldsymbol{z}_h, \boldsymbol{w}) \tag{7}$$

where

$$\boldsymbol{a}(\boldsymbol{z}; \boldsymbol{v}, \boldsymbol{w}) = \frac{\partial}{\partial \varepsilon} \boldsymbol{f}(\boldsymbol{z} + \varepsilon \boldsymbol{v}, \boldsymbol{w}) \Big|_{\varepsilon=0} = \boldsymbol{f}'(\boldsymbol{z}; \boldsymbol{v}, \boldsymbol{w}). \tag{8}$$

Again linearizing about $\boldsymbol{z}_h$ and neglecting high order terms, the error in a linear functional defined by the duality pairing $(\boldsymbol{\psi}, \cdot)$ can be written as

$$(\boldsymbol{\psi}, \boldsymbol{e}) = \boldsymbol{a}(\boldsymbol{z}_h; \boldsymbol{e}, \boldsymbol{\phi}) = -\boldsymbol{f}(\boldsymbol{z}_h, \boldsymbol{\phi}) \tag{9}$$

where $\boldsymbol{\phi}$ is the solution to the adjoint problem

$$\boldsymbol{a}(\boldsymbol{z}_h; \boldsymbol{w}, \boldsymbol{\phi}) = (\boldsymbol{\psi}, \boldsymbol{w}), \quad \forall \boldsymbol{w} \in \boldsymbol{V}. \tag{10}$$

Given $\boldsymbol{\phi}$ the error representation Eq. 9 is easily evaluated. However, usually the solution to the adjoint problem Eq. 10 is not given explicitly and we must approximate the solution using an appropriate discretization. In Drekar::CFD, we solve the adjoint problem using a finite element method with a higher-order approximation than we use for the forward problem. We remark that the same finite element space is often used for both the forward and adjoint problems [2, 1]. This approach requires the adjoint solution to be enriched via projection into a higher-order space. In general, it is difficult to prove that enriching the adjoint solution results in a more accurate approximation. It is generally accepted that solving the adjoint problem using a higher-order discretization results in more accurate error estimates.

2.4 Stabilized Formulations

We assume that the variational formulation (6) is sufficiently difficult to solve due to the structure of the operator itself or due to the choice of discrete subspace, and requires some form of stabilization to obtain a stable and accurate solution on practical grids.

Let $\mathscr{T}_h$ be a conforming partition of Ω, composed of N_T closed convex volumes of maximum diameter h. An element of the partition $\mathscr{T}_h$ will be denoted by T_i where h_i stands for the diameter of T_i for $i = 1, 2, \ldots, N_T$. We assume that the mesh is regular in the sense of Ciarlet [7]. We assume $\mathscr{T}_h$ is a conforming finite element mesh consisting of simplices or parallelopipeds. For convenience, we will use $(\cdot,\cdot)_{\mathscr{T}_h}$ to denote the inner product defined by,

$$(\boldsymbol{z}, \boldsymbol{w})_{\mathscr{T}_h} = \sum_{T_i \in \mathscr{T}_h} (\boldsymbol{z}, \boldsymbol{w})_{T_i}.$$

We define the stabilized weak formulation seeking $\boldsymbol{z} \in \boldsymbol{V}$ such that

$$\boldsymbol{f}_{\boldsymbol{\tau}}(\boldsymbol{z}, \boldsymbol{w}) = \boldsymbol{0}, \quad \forall \boldsymbol{w} \in \boldsymbol{V}, \tag{11}$$

where

$$\boldsymbol{f}_{\tau}(\boldsymbol{z}, \boldsymbol{w}) = \boldsymbol{f}(\boldsymbol{z}, \boldsymbol{w}) + (\boldsymbol{\tau}(\boldsymbol{z})\boldsymbol{F}(\boldsymbol{z}), \mathscr{P}(\boldsymbol{z})\boldsymbol{w})_{\mathscr{T}_h}, \tag{12}$$

and we assume $\boldsymbol{\tau}(\boldsymbol{z})$ is a diagonal matrix that may depend on $\boldsymbol{z}$ and may vary between elements but is typically constant within an element, see e.g. [17, 19, 8]. Note again that the variational residual $\boldsymbol{f}_{\tau}$ is linear in $\boldsymbol{w}$. A number of standard stabilization schemes can be defined by an appropriate choice of $\mathscr{P}(\boldsymbol{z})$. The discretized version of (11) seeks $\boldsymbol{z}_h \in \boldsymbol{V}_h$ such that

$$\boldsymbol{f}_{\boldsymbol{\tau}}(\boldsymbol{z}_h, \boldsymbol{w}) = \boldsymbol{0}, \quad \forall \boldsymbol{w} \in \boldsymbol{V}_h \tag{13}$$

where this statement is equivalent to Galerkin orthogonality.

A derivation similar to the variational form above, can be used to derive the adjoint of the stabilization, yielding the adjoint problem

$$\boldsymbol{a}_{\boldsymbol{\tau}}(\boldsymbol{z}_h; \boldsymbol{w}, \boldsymbol{\phi}_{\boldsymbol{\tau}}) = (\boldsymbol{\psi}, \boldsymbol{w}), \quad \forall \boldsymbol{w} \in \boldsymbol{V} \tag{14}$$

where

$$\boldsymbol{a}_{\boldsymbol{\tau}}(\boldsymbol{z}; \boldsymbol{v}, \boldsymbol{w}) = \frac{\partial}{\partial \varepsilon} \boldsymbol{f}_{\boldsymbol{\tau}}(\boldsymbol{z} + \varepsilon \boldsymbol{v}, \boldsymbol{w})|_{\varepsilon=0}. \tag{15}$$

An alternate path to derive an adjoint problem is to stabilize the strong form adjoint operator. This is beyond the scope of this work, but may be the subject of future investigation.

2.5 Navier-Stokes

We set $\boldsymbol{z} = (\boldsymbol{u}, p)^T$ to maintain the same notation from the previous section. The Navier-Stokes equations are given by,

$$\boldsymbol{F}(\boldsymbol{z}) = \boldsymbol{0},$$

where

$$\boldsymbol{F}(\boldsymbol{z}) = \begin{pmatrix} -\nu \Delta \boldsymbol{u} + \boldsymbol{u} \cdot \nabla \boldsymbol{u} + \nabla p - \boldsymbol{g}_{\boldsymbol{u}} \\ \nabla \cdot \boldsymbol{u} \end{pmatrix},$$

with appropriate boundary conditions. We assume that ν is sufficiently large so that a steady solution is expected. Of course, time-dependent approximation are also of interest, but this is beyond the scope of this paper.

The weak formulation of the Navier Stokes equations seeks $\boldsymbol{z} \in \boldsymbol{V} = \boldsymbol{H}^1(\Omega) \times L^2(\Omega)$ such that,

$$\boldsymbol{f}(\boldsymbol{z}, \boldsymbol{w}) = \boldsymbol{0}, \quad \forall \boldsymbol{w} \in \boldsymbol{V}, \tag{16}$$

where $\boldsymbol{w} = (\boldsymbol{v}, q)^T$ and

$$\boldsymbol{f}(\boldsymbol{z}, \boldsymbol{w}) = (\nu \nabla \boldsymbol{u}, \nabla \boldsymbol{v}) + (\boldsymbol{u} \cdot \nabla \boldsymbol{u}, \boldsymbol{v}) - (p, \nabla \cdot \boldsymbol{v}) + (\nabla \cdot \boldsymbol{u}, q) - (\boldsymbol{g}_{\boldsymbol{u}}, \boldsymbol{v}).$$

We consider equal order interpolation for the velocity and the pressure. For simplicity, we focus on Streamline Upwind Petrov-Galerkin stabilization (SUPG) with the pressure-stabilized Petrov-Galerkin (PSPG). The corresponding stabilization operator is given by,

$$\mathscr{P}(\boldsymbol{z})\boldsymbol{w} = \begin{pmatrix} \boldsymbol{u} \cdot \nabla \boldsymbol{v} + \nabla q \\ \nabla \cdot \boldsymbol{v} \end{pmatrix}. \tag{17}$$

It is straightforward to include a least-squares stabilization term on the incompressibility constraint (LSIC) or a discontinuity capturing stabilization (DCO) term.

3 Drekar Implementation

Drekar::CFD is a massively parallel unstructured fully-implicit (or semi-implicit) finite element Navier-Stokes solver build upon Trilinos [18]. The automatic differentiation tools allow for rapid code development and a straightforward implementation of advanced capabilities such as embedded uncertainty quantification and adjoints.

One of the challenges in goal-oriented a posteriori error estimation is the fact that the adjoint solution needs to be approximated using a finer discretization than was used for the forward problem. Occasionally we can to use the same approximation for the forward and adjoint problems, but this requires that the adjoint solution be projected into a finer space. While this is appealing from a computational perspective, in general it is difficult to define such projection operators and consequently the error estimate are often inaccurate. The numerical results in this report use piecewise linear Galerkin finite elements with SUPG stabilization to solve the forward problem and a higher-order (quadratic) finite element approximation with stabilization to solve the adjoint problem. Using a higher order approximation to solve the adjoint is generally regarded as the most robust approach to obtain accurate error estimates. The increase in computational cost associated with the higher-order basis functions is somewhat mitigated by the fact that the adjoint problem is linear.

We summarize the initial implementation of the adjoint-based error estimates in Drekar::CFD in Algorithm 3. We remark that it is possible to modify the above algorithm in a number of ways. Some of these include:

- Solving the adjoint problem with a low order method and computing a (nontrivial) projection of the adjoint approximation into a higher order space. Note that this is not the same projection as was used to compute $\boldsymbol{z}_H$.
- Deriving and discretizing a variational adjoint. Experience indicates that this is more robust than the discrete approach in Algorithm 3, but is more intrusive.
- Linearizing the adjoint around something other than the approximation of the forward problem. This is especially appealing for time-dependent problems.
- Computing the error representation an a weak residual integrated over the mesh. This is more useful for adaptive mesh refinement.

The Drekar::CFD implementation has been designed to be flexible enough to allow all of these modifications in the near future.

Algorithm 1 Computation of the a posteriori Error Estimate

Given low order and high order approximation spaces: $\boldsymbol{V}_L$ and $\boldsymbol{V}_H$ respectively.
Given a low order approximation of the forward solution, $\boldsymbol{z}_L \in \boldsymbol{V}_L$ satisfying

$$\boldsymbol{f}_{\boldsymbol{\tau}}(\boldsymbol{z}_L, \boldsymbol{v}_L) = 0, \quad \forall \boldsymbol{v}_L \in \boldsymbol{V}_L.$$

Given a QofI defining adjoint data:

$$\boldsymbol{\psi}_H = (\boldsymbol{\psi}, \boldsymbol{v}_H), \quad \forall \boldsymbol{v}_H \in \boldsymbol{V}_H.$$

Project forward approximation into higher order space (usually trivial):

$$\mathscr{P}\boldsymbol{z}_L = \boldsymbol{z}_H.$$

Compute residual of forward problem in higher order space:

$$\boldsymbol{r}_H = -\boldsymbol{f}_{\boldsymbol{\tau}}(\boldsymbol{z}_H, v_H), \quad \forall \boldsymbol{v}_H \in \boldsymbol{V}_H.$$

Compute adjoint of Jacobian in higher order space such that:

$$\boldsymbol{J}_H^T \boldsymbol{\phi}_H = \boldsymbol{a}_{\boldsymbol{\tau}}(\boldsymbol{z}_H; \boldsymbol{v}_H, \boldsymbol{\phi}_H), \quad \forall \boldsymbol{v}_H \in \boldsymbol{V}_H.$$

Solve the adjoint problem:

$$\boldsymbol{J}_H^T \boldsymbol{\phi}_H = \boldsymbol{\psi}_H.$$

Compute the error estimate as a weighted residual:

$$(\boldsymbol{\psi}, \boldsymbol{e}) = (\boldsymbol{r}_H, \boldsymbol{\phi}_H).$$

4 Computational Experiments

4.1 Channel Flow

In this section, we present numerical results for a two-dimensional laminar flow in a channel with an analytical solution. While this problem is rather simplistic, it does provide an opportunity to verify the adjoint solutions and the a posteriori error estimates. The computational domain is $[0,5] \times [0,1]$. Along the top and the bottom of the domain we enforce no-slip ($\boldsymbol{u} = \mathbf{0}$) boundary conditions. The left and right boundaries are inflow and outflow boundaries respectively. We set $u_y = 0$ along the inflow and the outflow. The flow is driven by a forcing term,

$$\boldsymbol{g_u} = \begin{pmatrix} 1 \\ 0 \end{pmatrix},$$

which acts as a pressure gradient. This problem has an analytical solution that depends on the kinematic viscosity. The magnitude of the velocity vector for $\nu = 1\text{E-}3$ is shown in Figure 1. The

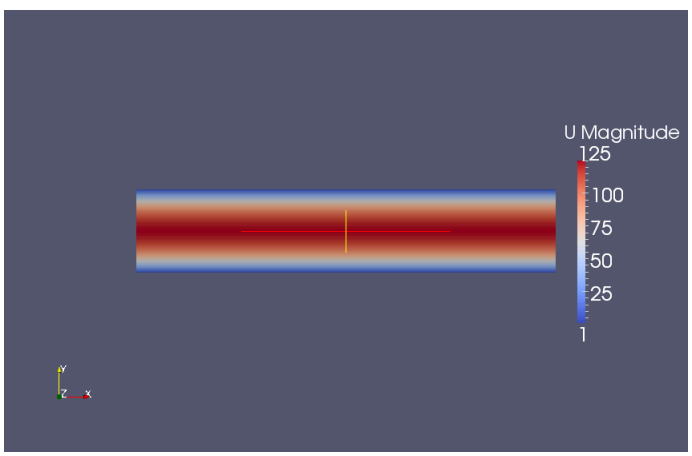

Figure 1. Magnitude of the forward velocity for the channel verification problem.

x-velocity follows a parabolic profile, the y-velocity is zero, and the pressure is zero.

To discretize, we partition the computational domain into 2000 uniform quadrilateral (square) elements. The forward problem is solved using piecewise linear finite elements with SUPG and PSPG stabilization. The adjoint problem is solved using Algorithm 3 with piecewise quadratic finite elements. The adjoint data, $\boldsymbol{\psi}$, is determined by the quantity of interest. We use $\boldsymbol{\psi}_x$, $\boldsymbol{\psi}_y$, and $\boldsymbol{\psi}_z$ to denote the x, y, and z components of $\boldsymbol{\psi}$ respectively. Since u_y and the pressure field can be represented exactly in the finite element space we are only interested in errors in u_x, we consider the following quantities of interest associated with u_x for verification:

1. The average value of the x-velocity for which

$$\boldsymbol{\psi}_x = 1/5.$$

2. The value of the x-velocity at $(4, 1/2)$ for which

$$\boldsymbol{\psi}_x = \delta_{(4,1/2)} \approx \frac{400}{\pi} \exp(-400(x-4)^2 - 400(y-1/2)^2).$$

3. The average value of the x-velocity over $[3,4] \times [0,1]$ for which

$$\boldsymbol{\psi}_x = \chi_{[3,4]\times[0,1]} = \begin{cases} 1, & (x,y) \in [3,4] \times [0,1], \\ 0, & \text{otherwise.} \end{cases}$$

In Table 1, we provide the estimate of the functionals, the a posteriori error estimates, and the effectivity ratios defined by

$$\text{Effectivity Ratio} = \frac{\text{Estimated Error}}{\text{True Error}}.$$

We observe that the effectivity ratios are nearly one for all three quantities of interest and both

QofI	Re	Estimated Value	Estimated Error	Effectivity Ratio
1	10	8.3125E-1	2.0833E-3	1.000
2	10	1.2385E+0	2.0779E-3	0.997
3	10	8.3125E-1	2.0833E-3	1.000
1	1000	8.3125E+1	2.0833E-1	1.000
2	1000	1.2385E+2	2.0779E-1	0.997
3	1000	8.3125E+1	2.0833E-1	1.000

Table 1. Error estimates and effectivity ratios for the three quantities of interest with Re= 10 and Re=1000.

Reynolds numbers. We note that the functional values and error estimates depend on the viscocity since the forward solution depends only the viscocity. However, the adjoint solutions may vary drastically for different Reynolds numbers. For comparison, in Figure 2 we plot the magnitude of the adjoint velocity corresponding to QofI 2 for Re= 10 (left) and for Re=1000 (right). We see that for the lower Reynolds number the domain of dependence, indicated by the support of the adjoint solution, is relatively close to the point (4,1/2). Meanwhile, the domain of dependence for the higher Reynolds number is mainly along the top, bottom, and inflow boundaries.

For another comparison, in Figure 3 we plot the adjoint pressure corresponding to QofI 1 (left) and QofI 3 (right) with Re= 10. Despite the fact that the two functional values are the same, the adjoint solutions are again quite different.

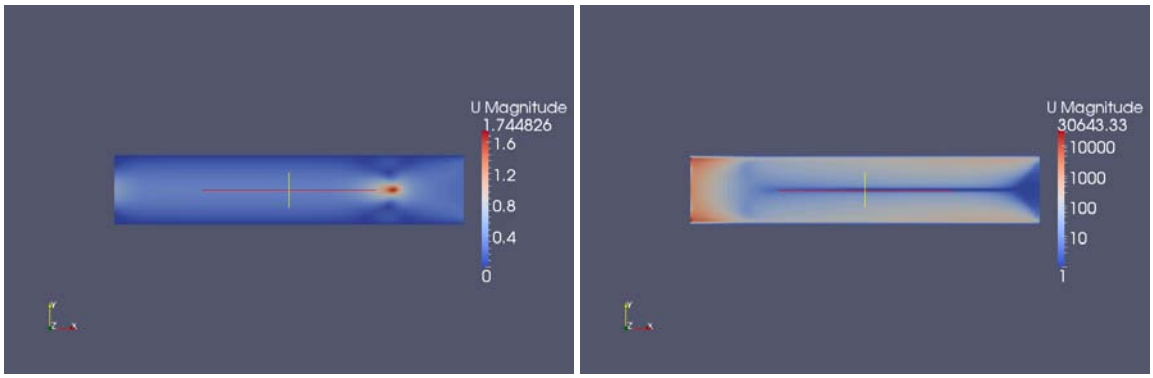

Figure 2. Magnitude of the adjoint velocity corresponding to QofI 2 for Re= 10 (left) and for Re=1000 (right).

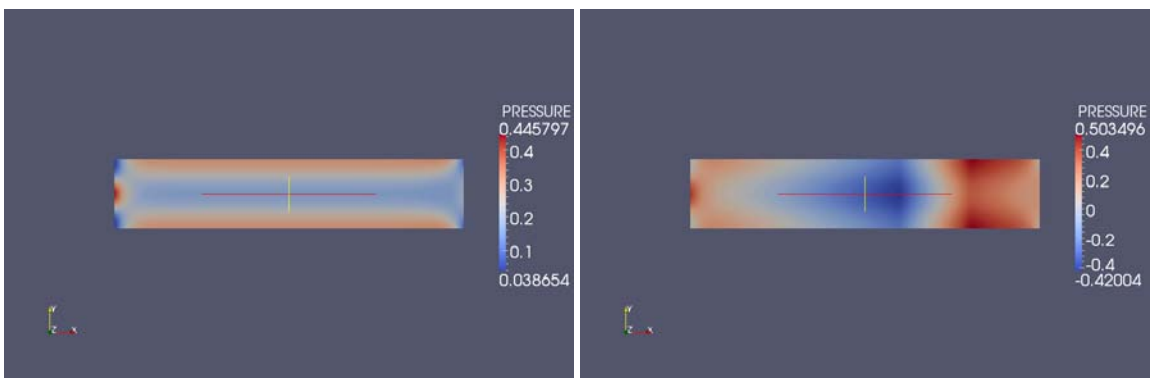

Figure 3. The adjoint pressure for Re= 10 corresponding to QofI 1 (left) and to QofI 3 (right).

4.2 Axisymmetric Expansion

In this section, we consider the axisymmetric sudden expansion problem (Benchmark #2 from TH-M). The computational domain consists of two cylinders of different radii as shown in Figure 4. The flow is in the z-direction and we do not consider the case with swirl. The mesh has 112,000 elements and 115,539 nodes. We solve the forward problem using a stabilized continuous Galerkin method with piecewise linear basis functions reulting in 115,539 degrees of freedom per equation. The adjoint problem uses piecewise quadratic basis functions and thus requires 910,597 degrees of freedom per equation. The significant increase in degrees of freedom for the adjoint problem did not pose a problem for the linear solver since the physics based algebraic multigrid preconditioner performed well in all simulations. The main challenge in solving the adjoint problem was due to the increased memory requirements to assemble and store the adjoint Jacobian which was much

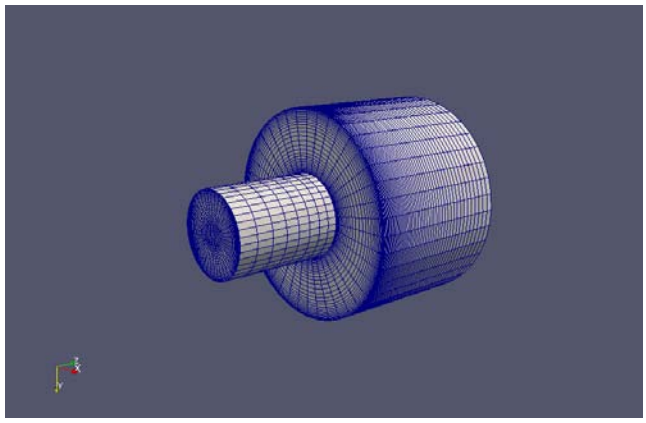

Figure 4. Computational mesh for the axisymmetric sudden expansion problem.

denser than the Jacobian of the forward problem. Thus, all of the numerical results were obtained using the Redsky capacity machine at Sandia National Laboratories on 128, 256 or 512 cores.

We solve the steady-state Navier Stokes equations with an inflow velocity and viscocity chosen so that the Reynolds number is about 500. We define the outflow boundary condition to be stress-free (natural outflow condition) and we enforce no-slip boundary conditions on the remaining boundaries. The magnitude of the forward velocity is shown in Figure 5.

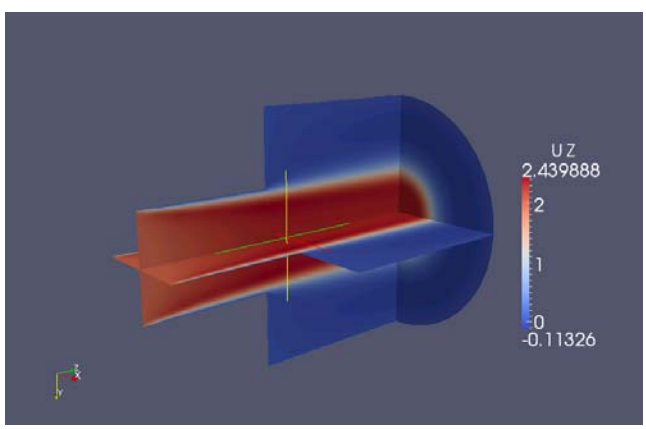

Figure 5. Magnitude of the forward velocity corresponding to Re= 500.

We consider the following quantities of interest:

1. The value of the x-velocity near $(0,0,0)$ for which

$$\boldsymbol{\psi}_x = \delta_{(0,0,0)} \approx 1000\exp(-100x^2 - 100y^2 - 100z^2).$$

2. The value of the y-velocity near $(0,0,0)$ for which

$$\boldsymbol{\psi}_y = \delta_{(0,0,0)} \approx 1000\exp(-100x^2 - 100y^2 - 100z^2).$$

3. The average value of the z-velocity over the domain for which

$$\boldsymbol{\psi}_z = 1/|\Omega|.$$

4. The value of the z-velocity at $(0,0,0)$ for which

$$\boldsymbol{\psi}_y = \delta_{(0,0,0)} \approx 2500\exp(-400x^2 - 400y^2 - 400z^2).$$

5. The value of the z-velocity at $(0.03,0,0)$ for which

$$\boldsymbol{\psi}_y = \delta_{(0,0,0)} \approx 2500\exp(-400(x-0.03)^2 - 400y^2 - 400z^2).$$

The exact solution is unknown, but the steady-state solution is symmetric, so the first two quantities of interest are zero for the true solution. In Table 2, we provide the estimated value of each QofI and the corresponding a posteriori error estimates. The accuracy of the a posteriori

QofI	Estimated Value	Estimated Error
1	-1.04775E-8	1.04799E-8
2	9.42114E-8	-9.41261E-8
3	3.07790E-4	1.05231E-8
4	4.68525E-1	-4.52085E-5
5	-2.34560E-3	1.22767E-6

Table 2. Error estimates for the quantities of interest for the axisymmetric sudden expansion problem.

error estimate for the first two quantities of interest indicates that the adjoint problem and error estimate have been implemented correctly for this problem. Exact values are not known for the other quantities of interest, but the error estimates are certainly plausible. In Figures 6, 7, and 8 we plot the adjoint solution for three different quantities of interest. These three examples do not necessarily correspond to the quantities of interest described above, but were chosen based on the adjoint solutions. Intuitively, the regions of the domain where the adjoint solution is nonzero provides an effective domain of dependence for the quantity of interest.

Next, we use a Reynolds Averaged Navier Stokes (RANS) model to approximate a steady solution to the problem described above at a higher Reynolds number. We use a Spalart-Allmaras

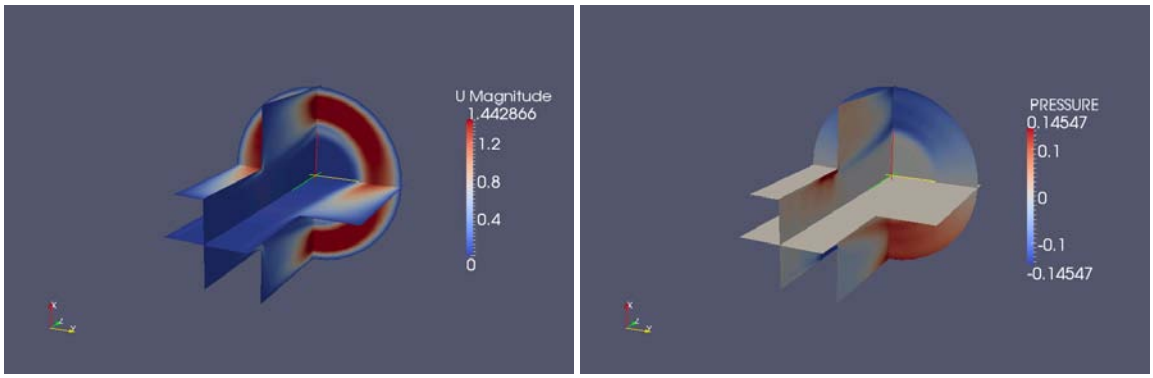

Figure 6. Magnitude of the adjoint velocity (left) and the adjoint pressure (right) corresponding to the average x-velocity over the domain.

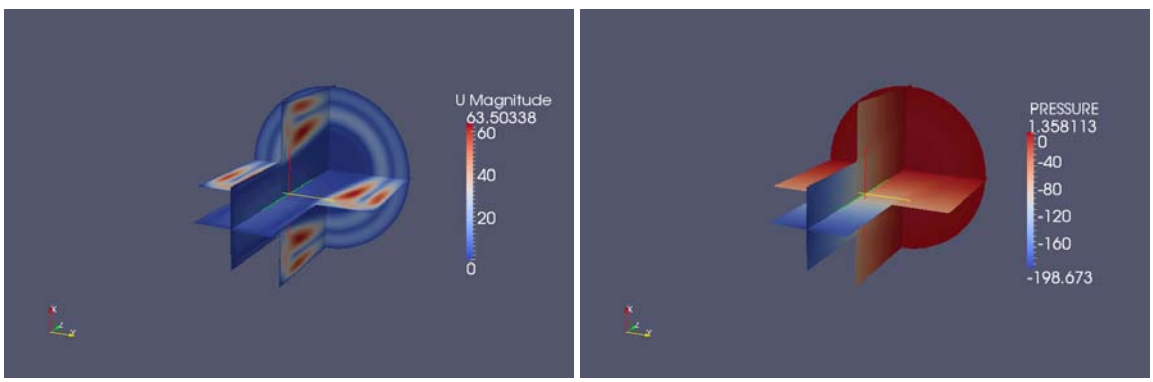

Figure 7. Magnitude of the adjoint velocity (left) and the adjoint pressure (right) corresponding to the value of the z-velocity at (0,0,0).

RANS model which requires the solution of a time-dependent advection-diffusion-reaction equation to approximate the turbulent viscocity. We choose an inflow velocity and kinematic viscosity to give a Reynolds number around 2500. We integrate the forward problem in time until a steady state is reached. Then we solve the steady state adjoint and compute an a posteriori error estimate using Algorithm 3.

Since the SARANS simulations are much more expensive in terms of computational cost than the Navier Stokes simulations, we only have an error estimate for one of the quantities of interest. This information is provided in Table 3. As in the previous case, the exact solution is unknown but the functional values and the error estimates appear plausible. Future work will compare these error estimates with mesh refinement studies.

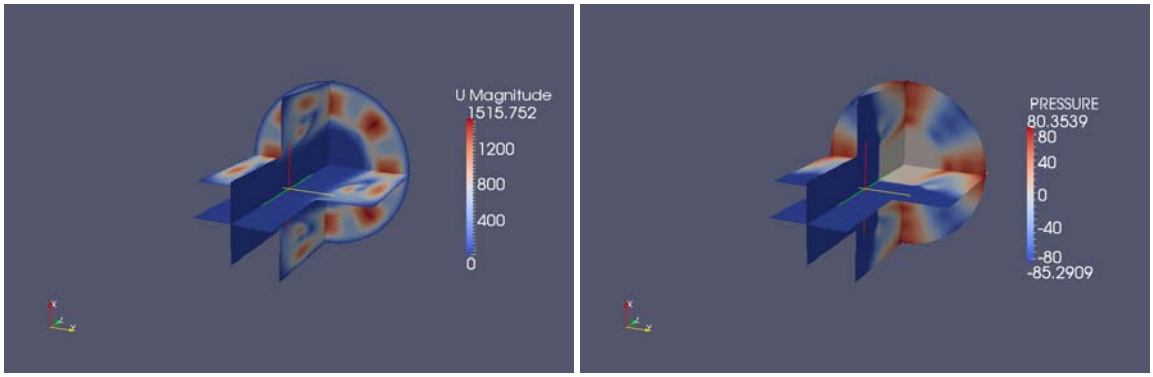

Figure 8. Magnitude of the adjoint velocity (left) and the adjoint pressure (right) corresponding to the average value of the z-velocity over $[-0.03, 0.03] \times [-0.03, 0.03] \times [0.02, 0.03]$..

QofI	Estimated Value	Estimated Error
4	1.96138E-1	-1.53864E-4

Table 3. Error estimates for a quantity of interest using an SA-RANS approximation of the axisymmetric sudden expansion problem.

5 Observations

- Drekar::CFD provides a flexible and extensible computational environment that easily facilitated the development of a framework for adjoint simulations and a posteriori error estimates.
- The framework developed utilizes the automatic differentiation and multiphysics assembly tools in Drekar::CFD to compute discrete adjoints for general nonlinear steady-state problems.
- Sensitivity of the quantity of interest with respect to parameter variations is easily computed using the same framework. This does not require a higher order approximation of the adjoint.
- The a posteriori error estimates have been verified using an analytical solution.
- A demonstration of these capabilities on a physically relevant problem with a steady-state model indicate that this approach may be feasible for verification of the CASL test problems and certainly warrants further investigation.
- Unfortunately, only one of the steady-state simulations using a RANS model is complete at this time. This is mainly due to difficulties in obtaining steady-state solutions for high Reynolds number flows and to the memory requirements for the high-order approximations. Work is in progress to ease these memory requirements using multilevel/multifidelity Jacobian-free Newton Krylov methods.
- Future work will also include a comparison of these a posteriori error estimates with the verification exercises performed in other VUQ and TH-M milestones.
- Extension of the adjoint framework to time-dependent nonlinear problems is of interest and may be pursued in FY13.

References

[1] W. Bangerth and R. Rannacher. *Adaptive Finite Element Methods for Differential Equations*. Birkhauser Verlag, 2003.

[2] Roland Becker and Rolf Rannacher. An optimal control approach to a posteriori error estimation in finite element methods. *Acta Numer.*, 10:1–102, 2001.

[3] J. Breidt, T. Butler, and D. Estep. A measure-theoretic computational method for inverse sensitivity problems I: Method and analysis. *SIAM J. Numer. Anal.*, (5):1836–1859, 2011.

[4] T. Butler, C. Dawson, and T. Wildey. A posteriori error analysis of stochastic differential equations using polynomial chaos expansions. *SIAM J. Scientific Computing*, 33(3):1267–1291, 2011.

[5] T. Butler, D. Estep, and J. Sandelin. A measure-theoretic computational method for inverse sensitivity problems II: A posterior error analysis. *SIAM J. Numer. Anal.*, 2011. to appear.

[6] V. Carey, D. Estep, and S. Tavener. *A posteriori* analysis and adaptive error control for multiscale operator decomposition solution of elliptic systems I: Triangular systems. *SIAM J. Numer. Anal.*, (47):740–761, 2009.

[7] P. G. Ciarlet. Basic error estimates for elliptic problems. In *Handbook of numerical analysis, Vol. II*, pages 17–351. North-Holland, Amsterdam, 1991.

[8] Ramon Codina. On stabilized finite element methods for linear systems of convectiondiffusion-reaction equations. *Computer Methods in Applied Mechanics and Engineering*, 188(13):61 – 82, 2000.

[9] K. Eriksson, D. Estep, P. Hansbo, and C. Johnson. *Computational differential equations*. Cambridge University Press, Cambridge, 1996.

[10] D. Estep. A posteriori error bounds and global error control for approximation of ordinary differential equations. *SIAM J. Numer. Anal.*, 32(1):1–48, 1995.

[11] D. Estep, V. Ginting, J. Shadid, and S. Tavener. An a posteriori-a priori analysis of multiscale operator splitting. *SIAM J. Numer. Anal.*, 46:1116–1146, 2008.

[12] D. Estep, M. G. Larson, and R. D. Williams. Estimating the error of numerical solutions of systems of reaction-diffusion equations. *Mem. Amer. Math. Soc.*, 146(696):viii+109, 2000.

[13] D. Estep and D. Neckels. Fast and reliable methods for determining the evolution of uncertain parameters in differential equations. *J. Comput. Phys.*, 213:530–556, 2006.

[14] D. Estep and D. Neckels. Fast methods for determining the evolution of uncertain parameters in reaction-diffusion equations. *Comput. Methods Appl. Mech. Engrg.*, 196:3967–3979, 2007.

[15] D. Estep, S. Tavener, and T. Wildey. *A posteriori* analysis and improved accuracy for an operator decomposition solution of a conjugate heat transfer problem. *SIAM J. Numer. Anal.*, 46:2068–2089, 2008.

[16] D. Estep, S. Tavener, and T. Wildey. A posteriori error estimation and adaptive mesh refinement for a multiscale operator decomposition approach to fluid-solid heat transfer. *J. Comput. Phys.*, 229:4143–4158, June 2010.

[17] Leopoldo P. Franca, Sérgio L. Frey, and Thomas J. R. Hughes. Stabilized finite element methods. I. Application to the advective-diffusive model. *Comput. Methods Appl. Mech. Engrg.*, 95(2):253–276, 1992.

[18] Michael Heroux, Roscoe Bartlett, Vicki Howle Robert Hoekstra, Jonathan Hu, Tamara Kolda, Richard Lehoucq, Kevin Long, Roger Pawlowski, Eric Phipps, Andrew Salinger, Heidi Thornquist, Ray Tuminaro, James Willenbring, and Alan Williams. An Overview of Trilinos. Technical Report SAND2003-2927, Sandia National Laboratories, 2003.

[19] Thomas J.R. Hughes. Multiscale phenomena: Green's functions, the dirichlet-to-neumann formulation, subgrid scale models, bubbles and the origins of stabilized methods. *Computer Methods in Applied Mechanics and Engineering*, 127(14):387 – 401, 1995.

[20] L. Mathelin and O. P. Le Matre. Dual-based error analysis for uncertainty quantification in a chemical system. *PAMM*, 7(1):2010007–2010008, 2007.

DISTRIBUTION:

1	MS 1318	Brian M. Adams, 1441
3	MS 1318	Michael S. Eldred, 1441
1	MS 1318	James R. Stewart, 1441
3	MS 1318	Timothy M. Wildey, 1441
1	MS 1320	Eric C. Cyr, 1426
1	MS 1320	Thomas M. Smith, 1442
1	MS 1321	John N. Shadid, 1444
1	MS 0899	Technical Library, 9536 (electronic copy)

Sandia National Laboratories